

## Properties of Si doped (11-20) a-plane GaN grown with different buffer layers

Chilsung Jung<sup>a</sup>, Junghwan Hwang<sup>a</sup>, Geunho Yoo<sup>a</sup>, Daehong Min<sup>a</sup>, Yongwoo Ryu<sup>a</sup>, Seunghwan Moon<sup>a</sup>, Minho Kim<sup>a</sup>, Kwangbo Shim<sup>b</sup> and Okhyun Nam<sup>a\*</sup>

<sup>a</sup>LED Technology Center, Department of Nano-Optical Engineering, Korea Polytechnic University, Siheung 429-793, Korea

<sup>b</sup>Division of Materials Science and Engineering, Hanyang University, 17 Hangdang-dong, Seongdong-gu, Seoul 133-791, Korea

We studied the properties of Si doped (11-20) a-plane GaN with two different buffer layers. The crystal quality of a-plane GaN is improved when a multi buffer (MB) rather than a conventional buffer (CB) layer is used. To study the effect of Si doping, the SiH<sub>4</sub> flow rate was varied from 0.9 to 40 sccm. As the flow rate is increased, both the carrier concentration and mobility are observed to increase. This arises owing to a change in the dominant scattering mechanism from defect and ionized scattering. The temperature dependent hall measurements show that the change in the scattering mechanism from dislocation to phonon scattering results from differences in the crystal quality between the samples.

**Key words:** Nonpolar GaN, Si-doping, Scattering mechanism, Metalorganic chemical vapor deposition.

### Introduction

III-nitride semiconductors are widely used in opto and microelectronic devices. Among them, gallium nitride (GaN) is extensively used in light emitting diodes (LEDs) [1-2]. Until recently, these materials were mostly grown on c-plane [0001] sapphire. In the c-orientation, the internal spontaneous and strain-induced piezoelectric polarization effects produce strong electric fields at the heterointerfaces [3]. Such internal electric fields result in an increased quantum-confined stark effect (QCSE), which leads to degradation in the performance of the optoelectronic devices due to a decrease in the recombination efficiency [4-5]. To minimize the QCSE effect nonpolar GaN can be used [6-10]. The nonpolar GaN is two surfaces perpendicular to the c axis, which have equal number of the Ga and N atoms, thus forming the so-called nonpolar surface. Most of the studies carried out so far have focused on the growth of non-polar GaN [11-13]. To obtain high performance nonpolar light-emitting diodes with high crystal quality, high electron concentration and mobility must be achieved.

Generally, it is difficult to obtain high crystalline, smooth, a-plane GaN films on sapphire due to the high density of stacking faults (SFs) and threading dislocations (TDs). Dislocations act as scattering centers for charge carriers and can influence the device properties and degrade the electrical properties. The Ga vacancy, which also functions as a scattering center, is involved in

the yellow luminescence transition in n-type GaN [14-16]. In this paper, we report the relationship between the crystal quality and Si-doping of (11-20) a-plane GaN layers with different buffer layers grown on (1-102) r-plane sapphire via metal organic chemical vapor deposition (MOCVD).

### Experimental

Nonpolar a-plane GaN was grown on (1-102) r-plane sapphire substrates in a 3 × 2" Thomas Swan close coupled showerhead metalorganic chemical vapor deposition system. Trimethylgallium (TMGa) and ammonia (NH<sub>3</sub>) metal organic sources were used. Silane (SiH<sub>4</sub>) was used as the n-doping source. Prior to growth, the sapphire substrate was thermally cleaned and nitrided at 1090 °C under a mixture of H<sub>2</sub> and NH<sub>3</sub> gases. To grow a-plane GaN with varying crystal quality, two different buffer layers, a conventional buffer (CB) layer and a multi buffer (MB) layer, were used. The CB layer was grown on a sapphire substrate at 1050 °C under a N<sub>2</sub> atmosphere at 100 torr. The thickness of the layer was approximately 100 nm. The MB layer was grown under optimized growth conditions to obtain high quality a-plane GaN templates with a 1 μm -thick, 3-step GaN buffer layer. The first buffer layer was similar to the CB layer due to nucleation of the layer on the r-plane sapphire substrate. The second and third buffer layers were grown under slightly different conditions to reduce defect density and anisotropy. The second buffer layer was grown at a pressure of 70 torr so that the anisotropy could be controlled along the m-direction. The third buffer layer was grown at a pressure of 300 torr at 770 °C to allow three-dimensional growth. For subsequent growth of a-

\*Corresponding author:  
Tel : +82-31-8041-0718  
Fax: +82-31-8041-1917  
E-mail: ohnam@kpu.ac.kr

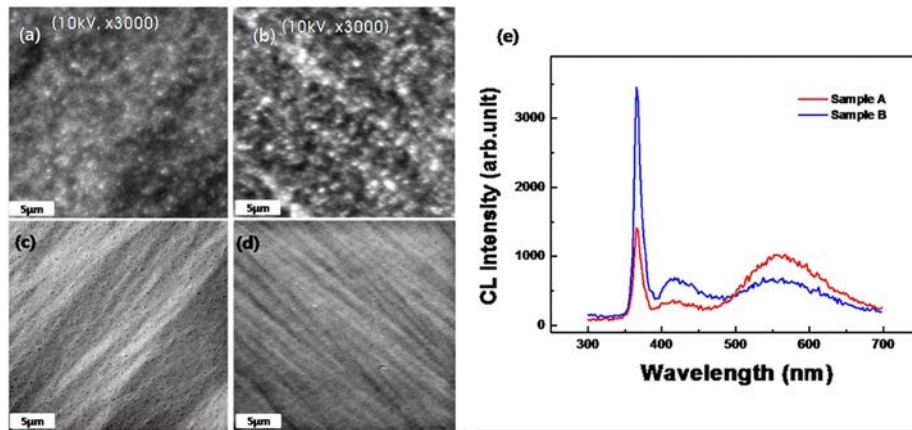


**Fig. 1.** The cathodoluminescence (CL) images [(a)-(b)], SEM images [(c)-(d)] and CL spectra (e) of sample A and sample B, respectively.

plane GaN on the MB layer, two dimensional growth of the GaN was observed [17-18]. A 2  $\mu\text{m}$  Si doped a-plane GaN film was then grown by adding  $\text{SiH}_4$  gas to the  $\text{H}_2$  atmosphere. The  $\text{SiH}_4$  flow rates used were 0.9, 3, 18, and 40 sccm. The surface morphologies of the samples were characterized using a scanning electron microscope (SEM) and the crystal quality was investigated by cathodoluminescence (CL) and high resolution X-ray diffraction (HRXRD) measurements. The carrier scattering mechanisms of the Si doped samples with different crystal qualities were analyzed using room temperature photoluminescence (PL), on- and off- axis X-ray rocking curves (XRCs), and temperature dependent Hall measurements.

## Results and Discussion

### Undoped a-plane GaN with different buffer layers

Figures 1(a) and (b) show the CL images of the undoped a-plane GaN with different CB (sample A) and MB (sample B) buffer layers. The corresponding SEM images are shown in figures 1(c) and (d), respectively. The CL image of sample B is brighter than that of sample A. In addition, the CL spectrum intensity of both samples reveals the same result that is shown in figure 1(e). The near band edge (NBE) emission intensity of sample B is 230% greater than that of sample A. Figure 2 shows the full width at half maximum (FWHM) of the X-ray rocking curve (XRC) for samples A and B at different azimuth angles. It has previously been reported that the morphological and structural anisotropy produced in a-plane GaN results from different growth rates along the c-direction and the m-direction [19-20]. The results show that sample A has a significant anisotropy of 960 arcsec at  $\phi = 0^\circ$  and 2680 arcsec at  $\phi = 90^\circ$ . The anisotropy in the FWHM of sample B is considerably lower at 660 arcsec at  $\phi = 0^\circ$  and 1300 arcsec at  $\phi = 90^\circ$ . This indicates that the crystal quality of sample B is better than that of sample A.

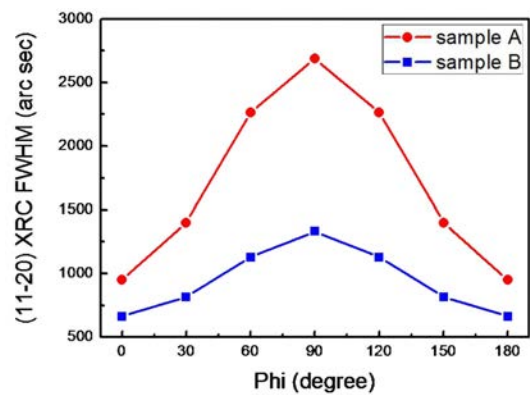


**Fig. 2.** The FWHMs of the on-axis XRCs of sample A and B as a function of the azimuth angle,  $\phi$ .

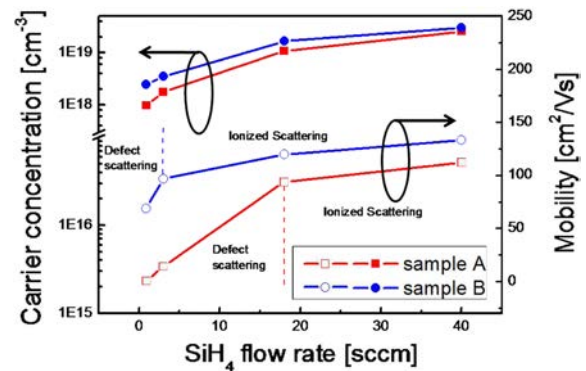


**Fig. 3.** Room temperature carrier concentration and mobility of both Si doped sample A and B with  $\text{SiH}_4$  flow rates.

### Si-doped a-plane GaN with different buffer layers

The room-temperature carrier concentration and mobility of a-plane GaN were studied for layers grown at different  $\text{SiH}_4$  flow rates. For Si doped c-plane GaN, the carrier mobility decreases with increasing  $\text{SiH}_4$  flow rate due to increased scattering from ionized impurities [21]. Figure 3 shows the carrier mobility of the Si doped a-plane GaN. The carrier mobility increases with increasing  $\text{SiH}_4$  flow rate. This increase is associated with defect scattering from the high

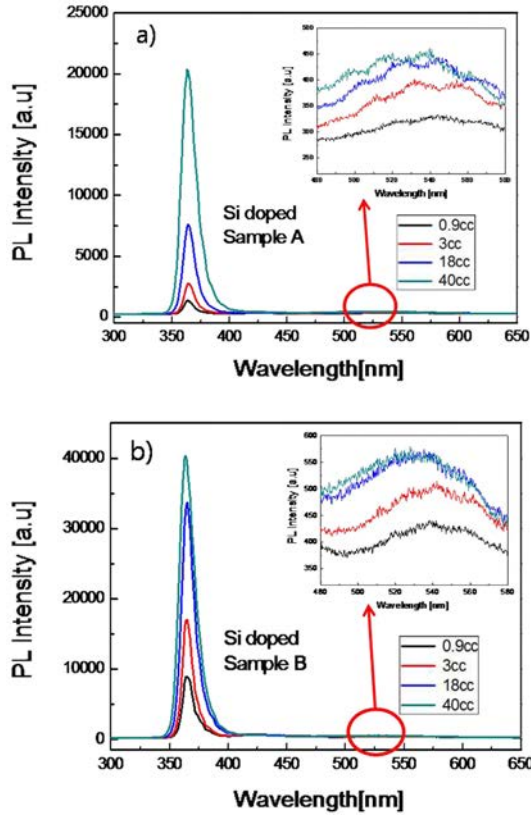


**Fig. 4.** Room temperature photoluminescence (PL) spectra of both Si-doped sample A (a) and B (b) with different  $\text{SiH}_4$  flow rates. The inset shows the peak of yellow luminescence (YL) emission with different  $\text{SiH}_4$  flow rates, respectively.

density of defects ( $1 \times 10^{10} \text{ cm}^{-2}$ ) in a-plane GaN. The carrier concentrations increase, with increasing  $\text{SiH}_4$  flow rate, from  $1 \times 10^{18}$  to  $1.5 \times 10^{19} \text{ cm}^{-3}$  and from  $2 \times 10^{18}$  to  $2 \times 10^{19} \text{ cm}^{-3}$  for samples A and B respectively. The carrier concentration and mobility are higher in sample B than sample A at any given  $\text{SiH}_4$  flow rate. This is probably due to a lower defect density in sample A.

The increasing mobility as a function of  $\text{SiH}_4$  flow rate is shown in figure 3. For sample A, the carrier mobility increases steeply as a function of flow rate until the flow rate reaches 18 sccm. This increase is due to increased defect scattering. The rate of increase in the mobility then slows down for flow rates above 18 sccm due to ionized scattering [21]. For flow rates up to 3 sccm, the carrier mobility increases faster for the Si doped sample B than for sample A. However, for higher flow rates the increase is much slower due to the low defect density in sample B.

Defect scattering occurs via two scattering mechanisms: vacancy scattering and dislocation scattering [22]. The defects act as scattering centers and can interrupt the carrier mobility. To look at the effects of vacancy scattering, the optical properties of Si doped a-plane GaN were studied using room temperature PL. The results are shown in figure 4. Both the near band edge

**Table 1.** The ratio of the intensity of NBE to YL of the Si-doped sample A and B with varied  $\text{SiH}_4$  flow rates.

	$I_{\text{NBE}}/I_{\text{YL}}$ (0.9 sccm)	$I_{\text{NBE}}/I_{\text{YL}}$ (3 sccm)	$I_{\text{NBE}}/I_{\text{YL}}$ (18 sccm)	$I_{\text{NBE}}/I_{\text{YL}}$ (40 sccm)
Sample A	4.1	6.8	17.1	44.3
Sample B	20.2	33.1	58.7	69.7

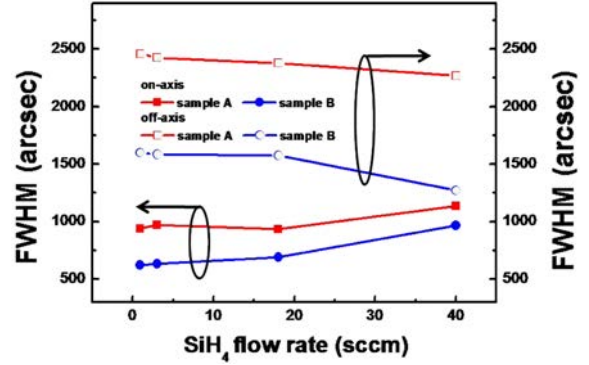


**Fig. 5.** The on (11-20) and off (10-11) axis XRC FWHM of Si doped sample A and B with different  $\text{SiH}_4$  flow rates.

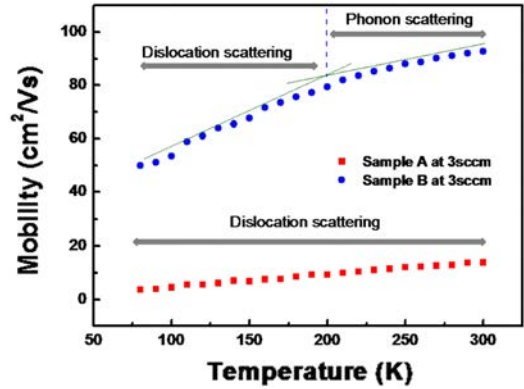


**Fig. 6.** The temperature dependence of electron mobility of Si doped sample A and B at 3 sccm  $\text{SiH}_4$  flow rate.

(NBE) and yellow luminescence (YL) emission (insets) intensity increase with increasing  $\text{SiH}_4$  flow rate. The ratio of  $I_{\text{NBE}}/I_{\text{YL}}$  was measured in order to understand how the crystal quality influences the YL emission. The  $I_{\text{NBE}}/I_{\text{YL}}$  ratios for samples A and B, grown under different flow rates, are shown in table 1. The  $I_{\text{NBE}}/I_{\text{YL}}$  ratio is higher for Si doped sample B with high crystal quality than for sample A for all  $\text{SiH}_4$  flow rates. It was previously reported that YL emission in a-plane GaN originates from the formation of Ga vacancy,  $V_{\text{Ga}}$  [14, 23]. The results in table 1 suggest that sample A has more  $V_{\text{Ga}}$  than sample B, since the  $I_{\text{NBE}}/I_{\text{YL}}$  ratio is lower. The  $V_{\text{Ga}}$  provides negatively charged Coulombic scattering centers in n-type a-plane GaN, which induce defect related scattering and reduce carrier mobility [23].

Figure 5 shows the FWHM of the XRC for the different Si doped (11-20) and (10-11) GaN samples. Ma *et al.* [12] reported that the FWHM values of on-axis (11-20) GaN increases slightly with Si doping.

Similar results are obtained here. The on-axis FWHM values are broadened by screw and mixed threading dislocations. However, the off-axis (10-11) GaN planes are broadened by edge-type dislocations [24]. The edge-type dislocation is well known for providing acceptor traps and forming negatively charged Coulombic scattering centers [21, 25]. The decrease in the FWHM with increasing SiH<sub>4</sub> flow rate for the off-axis (10-11) planes, as shown in figure 5, implies that the density of negatively charged Coulombic scattering centers decreases with increasing flow rate, which eventually leads to an increase in the mobility.

Figure 6 shows the temperature dependence of the electron mobility for Si doped samples grown at SiH<sub>4</sub> flow rates of 3 sccm. All the samples have similar low carrier concentrations of 10<sup>18</sup> cm<sup>-3</sup> (figure 3). The peak in the mobility occurs at 300 K for both samples. However, the peak in the mobility for samples A and B varies greatly from 12 to 93 cm<sup>2</sup>/Vs, respectively. This variation can be attributed to the difference in crystal quality between the two samples. At low temperatures, the mobility increases linearly with temperature. This is probably due to scattering by dislocations. The mobility of the Si doped sample B saturates at higher temperatures. This saturation is attributed to a change in the scattering mechanism from dislocation scattering to phonon scattering [12]. A change in the scattering mechanism is only observed for the Si doped sample B, suggesting that high crystal quality is required for high electrical properties.

### Conclusions

We investigated the properties of Si doped (11-20) a-plane GaN with two different buffer layers. The crystal quality of GaN was considerably improved when a multi buffer layer, rather than conventional buffer layer, was used. Both the carrier concentration and mobility were seen to increase with increasing SiH<sub>4</sub> flow rates. This behavior arises from a change in the dominant scattering mechanism from defect to ionized scattering, as shown by photoluminescence and X-ray rocking curve measurements. The change in the scattering mechanism from dislocation to phonon scattering was discussed in relation to the defect density as probed using temperature dependent hall measurements. The results show that to obtain high electrical properties Si doped a-plane GaN layers with low defect densities need to be grown.

### Acknowledgments

This work was supported by Industrial Strategic Technology Development Program No. 10041188 of the Ministry of Knowledge Economy and the National

Research Foundation of Korea (NRF) grant funded by the Korea government (MEST) (No. 2012R1A2A2A 01011702).

### References

1. S. Nakamura and G. Fasol: The Blue Laser Diode. Berlin. Springer. 1997.
2. S. J. Pearton, J. C. Zolper, R.J. Shul, and F. J. Ren: J. Appl. Phys. 86 (1999) 1.
3. F. Bernardini, V. Fiorentini, and D. Vanderbilt: Phys. Rev. B. 56 (1997) R10024.
4. T. Deguchi, K. Sekiguchi, A. Nakamura, T. Sota, R. Matsuo, M. Ramsteiner, M. Reiche, and K. H. Ploog: Nature. 406 (2000) 865-868.
5. T. Takeuchi, S. Sota, M. Katsuragawa, M. Komori, H. Takeuchi, H. Amono and I. Akasaki: Jpn. J. Appl. Phys. 36 (1997) 382-385.
6. X. Ni, Y. Fu, Y. T. Moon, N. Biyikli, and H. Morkoc: J. Cryst. Growth. 290 (2006) 166-170.
7. T. S. Ko, T. C. Wang, R. C. Gao, H. G. Chen, G.S. Huang, T.C. Lu, H.C. Kuo, and S.C. Wang: J. Cryst. Growth. 300 (2007) 308-313.
8. C. Chen, A. Vdivarahan, J. Yang, M. Shatalov, E. Kuokstis, and M. Asif Khan: Jpn. J. Appl. Phys. 42 (2003) L1039-L1040.
9. G. H. Yoo, H. S. Park, H. J. Lim, S. A. Lee, O. H. Nam, Y. B. Moon, C. R. Lim, B. H. Kong, and H. K. Cho: Jpn. J. Appl. Phys. 50 (2011) 042103-042103-3.
10. Yong Seok Lee, Tae Hoon Seo, Ah Hyun Park, Kang Jea Lee, Sang Jo Chung, and Eun-Kyung Suh: Electron. Mater. Lett. 8 (2012) 335-339.
11. K. Kusakabe, T. Furuzuki, K. Ohakawa: Physica B. 376 (2006) 520-522.
12. Bei Ma, Reina Miyagawa, Weiguo Hu, Da-bing Li, Hideto Miyake, Kazumasa Hiramatsu: J. Cryst. Growth. 311 (2009) 2902.
13. Keun Man Song, Chang Zoo Kim, Jong Min Kim, Dae Ho Yoon, Sung Min Hwang, and Hyoung Kim: Jpn. J. Appl. Phys. 50 (2011) 05502-05502-4.
14. H. B. Yu, G. Chen, Dongsheng, Li, Y. J. Han, X. H. Zheng, Q. Huang, and J. M. Zhou: J. Cryst. Growth. 263 (2004) 94-98.
15. D. C. Reynolds, D. C. Look, and B. Jogai: J. Appl. Phys. 88 (2000) 5760-5763.
16. D. Li, B. Ma, R. Miyagawa, W. Hu, M. Narukawa, H. Miyake, K. Hiramatsu: J. Cryst. Growth. 311 (2009) 2906-2909.
17. C. F. Johnston, M. J. Kappers and C. J. Humphreys: J. Appl. Phys. 105 (2009) 073102-073102-6.
18. S. M. Hwang, Y. G. Seo, K. H. Baik, I. S. Cho, J. H. Baek, S. Jung, T. G. Kim and M. Cho: Appl. Phys. Lett. 95 (2009) 071101-071101-3.
19. J. L. Hollander, M. J. Kappers, C. McAleese, and C. J. Humphreys: Appl. Phys. Lett. 92 (2008) 101104-101104-3.
20. Q. Sun, T. S. Ko, C. D. Yerino, Y. Zhang, I. H. Lee, J. Han, T. C. Lu, H. C. Kuo and S. C. Wang: Jpn. J. Appl. Phys. 48 (2009) 071002-071002-4.
21. H. M. Ng, D. Doppalaapudi, T. D. Moustakas, N. G. Weimann, and L. F. Eastman: Appl. Phys. Lett. 73 (1998) 821-823.
22. Xu ShengRui, Zhou XiaoWei, Hao Yue, Yang LiNam,

- Zhang JinCheng, Mao Wei, Yang Cui Cai Maoshi, Ou XinXiu, Shi LinYu, and Cao YanRong: *Sci. China. Tech. Sci.* 53 (2010) 2363-2366.
23. H.Z. Xu, A. Bell, Z.G. Wang, Y. Okada, M. Kawabe, I. Harrison, and C.T. Foxon: *J. Cryst. Growth.* 222 (2001) 96-103.
24. M. D. Craven, S. H Lim, F. Wu, J. S. Speck, and S. P. DenBaars: *Appl. Phys. Lett.* 81 (2002) 469-471.
25. N. G. Weimann, L. F. Eastman, D. Doppalapudi, H. M. Ng, and T. D. Moustakas: *J. Appl. Phys.* 83 (1998) 3656-3659.